Characterizing and Exploiting Partial Interference in Wireless Mesh Networks

Ka-Hung Hui, Wing-Cheong Lau and On-Ching Yue
Department of Information Engineering
The Chinese University of Hong Kong
Shatin, Hong Kong
Email: {khhui5, wclau, onching}@ie.cuhk.edu.hk

***Abstract*— In evaluating the performance of a wireless network, the interference between wireless links plays a key role. In previous works, interference was assumed to be a binary phenomenon, *i.e.*, either the links mutually interfere with each other, or they do not interfere. However, there were experimental results contradicting this binary assumption. We term this as *partial interference*. In this paper, we present an analytical framework to characterize partial interference in a single-channel wireless network under unsaturated traffic conditions, and use 802.11b with basic access scheme and differential binary phase shift keying as an illustration. An analogy is drawn between partial interference and code division multiple access to demonstrate their similarities. The gain in capacity across unit cut by exploiting partial interference can be as high as 67% under scheduling in a modified Manhattan network.**

I. Introduction

In an *ad hoc* wireless network, all stations communicate with each other through wireless links. A fundamental difference between a wireless network and its wired counterpart is that wireless links may *interfere* with each other, resulting in performance degradation. As a result, there have been numerous researches on wireless networks considering interference between wireless links.

The performance of wireless networks in terms of their capacities has received much attention. Several interference models were proposed [1] to predict whether transmissions in a wireless network are successful and derive the capacity of the wireless network. Other researchers used these models to calculate the capacity of a wireless network and compute the schedules to achieve it [2], [3], [4].

In these interference models, one key assumption is that interference is a *binary* phenomenon, *i.e.*, either the links mutually interfere with each other, or they do not interfere. However, it was reported that this assumption is not valid, both in single-channel [5] and multi-channel [6] scenarios, which means that it is possible for interfering links to be active simultaneously and realize some throughput. We term this as *partial interference*. This implies that the interference models used are overly simplified, and motivates us to develop more accurate models to capture this partial behavior.

In this paper, we make the following contributions:

1) In Sections III and IV we propose an analytical framework to characterize partial interference in a single-channel wireless network. We extend the Markov model in [7] to take into account the unsaturated traffic conditions, the signal-to-noise ratio (SNR) attained at the receivers and the modulation scheme employed. These modifications result in a *partial interference region*, implying that the interference models used in previous works are not accurate enough.
2) We provide an intuitive analogy in Section V between our results and time division multiple access (TDMA) with code division multiple access (CDMA) to explain our analytical results and illustrate the importance of carrier sensing threshold in our model.
3) We show in Section VI with an example that the gain in capacity across unit cut by exploiting partial interference can be as high as 67%. We also illustrate that there is a tradeoff between the *capacity* and the *density* of the links in a wireless network.

For the rest of the paper, we present the related works in Section II, and we conclude the paper and discuss future works in Section VII.

II. Related Works

In [1], two interference models, called the *protocol model* and the *physical model*, were introduced. The protocol model states that a transmission is successful if the corresponding receiver is located inside the transmission range of the transmitter, and all other active transmitters are located outside the interference range of the receiver. In the physical model, the transmissions from other transmitters are considered as noise, and a transmission is successful if the SNR attained at the receiver exceeds a certain threshold. Based on these models, the capacities of a multi-hop wireless network under random and optimal node placement were derived.

There have been various studies focusing on the capacity of a multi-hop wireless network in any given static topology. The capacity-finding problem was modeled as a maximum flow or a multi-commodity flow problem in graph theory [8]. Based on these interference models, the *independent sets* and the *schedulable sets* were proposed in [2] to formulate the maximum flow problem and compute the maximum throughput. Various ways to bound the maximum throughput were also proposed. In [3], the *row constraints* and the *clique constraints* were proposed to find the bounds of the maximum throughput obtained in [2]. In [4], the authors used the protocol model to

set up the multi-commodity flow problem in a multi-channel, multi-radio wireless mesh network and solve for the capacity.

In [5], the authors measured the interference among links in a single-channel, static 802.11 multi-hop wireless network. They measured the interference between pairs of links by the *link interference ratio*, and observed that this ratio exhibited a continuum between 0 and 1. In [6], two interfering links were set up in a wireless network with multiple partially overlapped channels to measure TCP and UDP throughputs of an individual link. It was found that the throughputs increased smoothly when the separation between the links increased. The throughputs increased more rapidly as the channel separation between the links increased. These experimental results suggest that the binary assumption in the protocol and the physical models may not be valid.

There have been some preliminary works on finding the relationship between the SNR attained at a receiver and the throughput achieved by the corresponding wireless link. In [9], a methodology for estimating the packet error rate in the *affected wireless network* due to the interference from the *interfering wireless network* was presented. The throughput of the affected wireless network was found to increase continuously with the SNR attained at the corresponding receiver, which increased with the separation between the networks.

One complication in finding the capacity of a wireless network is that we cannot assume the stations to operate in saturated conditions, otherwise the network will result in instability. Therefore, there have been some researches working on characterizing the *stability region* and the *capacity region* of a wireless network. In [10], the authors used *stochastic dominance* to obtain bounds on the stability region of a discrete-time slotted ALOHA system. In [11], the connection between the stability region and the capacity region of a wireless network was established, and the capacities of regular wireless networks were obtained. In these works, interference was still assumed to be binary.

III. System Model

We present our framework to characterize partial interference in a wireless network. In this framework, we derive the *transmission probabilities* τ_n and the *packet corruption probabilities* c_n of the links in the network. τ_n is the probability that a station transmits in a randomly chosen slot, while c_n is the probability that a packet is received with error.

A. Assumptions

For illustration, we choose the MAC and PHY protocols to be 802.11b with basic access scheme and 1Mbps differential binary phase shift keying (DBPSK). Our model can be readily extended to consider other modulation schemes. In addition, we make the following assumptions:

- The network consists of two links (T_1, R_1) and (T_2, R_2), where T_n and R_n denote the transmitter and the receiver of the links respectively, $n = 1, 2$.
- There are a constant *buffer nonempty probability* q_n that the transmission buffer of T_n is nonempty and a constant *channel idle probability* i_n that T_n senses the channel to be idle, $n = 1, 2$.
- T_n transmits with power P_n, and the background noise power at R_n is N_n, $n = 1, 2$.
- Channel defects like shadowing and fading are neglected, and a generic path loss model $pl(d) = Cd^{-\alpha}$ is used to model the wireless channel, where d is the propagation distance, α is the path loss exponent and C is a constant.
- The interference from other transmitters plus the receiver background noise is assumed to be Gaussian distributed.
- All bits in a packet must be received correctly for correct reception of the packet.
- The size of an acknowledgement is much smaller than that of the payload, so the bit errors on acknowledgement are negligible.

B. Transmission Probability Calculation

We follow the approach as in [7], using a discrete-time Markov chain to model the 802.11 Distributed Coordination Function (DCF) and obtain the transmission probability of a station. An ordered pair (j, k) is used to denote the state of the Markov chain, where j represents the backoff stage, and k is the current backoff counter value. In stage j, k is in the range $[0, W_j - 1]$, where W_j is the contention window size in stage j. m is the maximum number of backoff stages. However, there are some discrepancies between this model and the actual behavior of 802.11 DCF. First, the model assumes that a station retransmits indefinitely until the packet is successfully transmitted. This assumption is inconsistent with 802.11 basic access scheme. Also, the model does not account for the unsaturated traffic conditions, which is the scenario appeared in practical situations.

We adopt the following modifications on the Markov chain to obtain a better model. First, we take into account the limited number of retransmissions in 802.11 as in [12], by restricting the Markov chain to leave the m-th backoff stage once the station transmits a packet in that backoff stage. Second, we follow [12] to modify the values of W_j in accordance with the 802.11 MAC and PHY specifications [13], with m' corresponding to the first backoff stage using the maximum contention window size:

$$W_j = \begin{cases} 2^j W_0, & 0 \le j \le m' \\ 2^{m'} W_0, & m' < j \le m \end{cases}.$$

In addition, to model the unsaturated conditions, we follow [14] to augment the Markov chain by introducing new states $(-1, k), k \in [0, W_0 - 1]$. These new states represent the states of being in the post-backoff stage. The post-backoff stage is entered whenever the station has no packets queued in its transmission buffer after a successful transmission. The corresponding Markov chain is depicted in Fig. 1. Let $\pi_{j,k}$ denote the stationary probability of the state (j, k) in the Markov chain. The transmission probability of a station is

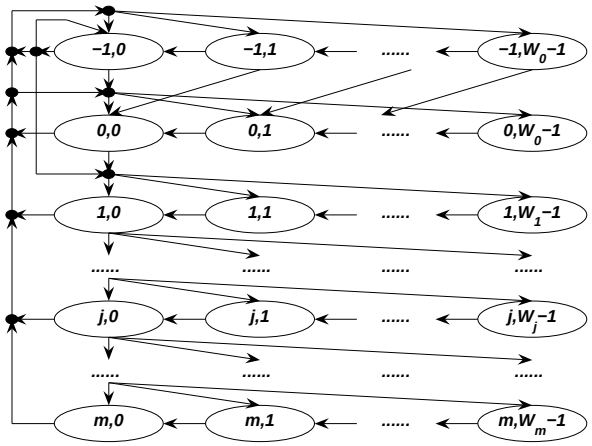

Fig. 1. A Markov chain model for 802.11 DCF in unsaturated conditions.

given by

$$\begin{aligned}\tau_n &= \pi_{-1,0} q_n i_n + \sum_{j=0}^{m} \pi_{j,0} \\ &= \left(2q_n^2 W_0 \sum_{j=0}^{m} c_n^j\right)\Bigg\{q_n^2 W_0 \sum_{j=0}^{m} c_n^j (W_j+1) \\ &\quad + (1-q_n)\Big[1-(1-q_n)^{W_0}\Big] \\ &\quad \times [q_n(1-i_n)(W_0+1) + 2(1-q_n)]\Bigg\}^{-1}. \end{aligned} \quad (1)$$

C. Packet Corruption Probability Calculation

The packet corruption probability is calculated according to the modulation scheme used in the PHY layer, the distance between the transmitter and the receiver, and the existence of nearby interferer(s). For a fixed *carrier sensing threshold* β, we differentiate into two cases, whether both transmitters can sense the transmission of each other or not.

If T_1 can sense the transmission of T_2, *i.e.*, $P_2 pl\big(d_{T_1,T_2}\big) > \beta$, where $d_{X,Y}$ is the distance between X and Y, then the SNR at R_1 is

$$\gamma_1 = \frac{P_1 pl\big(d_{T_1,R_1}\big)}{N_1}.$$

The bit error rate attained by (T_1, R_1) is $e(\gamma_1) = \frac{1}{2}\exp(-\gamma_1)$ [15], and the packet corruption probability for (T_1, R_1) is

$$c_1 = 1 - [1 - e(\gamma_1)]^{H_P + H_M + L}, \quad (2)$$

where H_P, H_M and L represent the number of bits in the PHY header, the MAC header and the payload respectively.

On the other hand, if T_1 cannot sense the transmission of T_2, *i.e.*, $P_2 pl\big(d_{T_1,T_2}\big) \le \beta$, then the SNR at R_1 depends on whether T_2 is active in transmission or not, *i.e.*,

$$\Pr\{\gamma_1 = \gamma\} = \begin{cases} 1-\tau_2, & \gamma = \dfrac{P_1 pl\big(d_{T_1,R_1}\big)}{N_1} \\ \tau_2, & \gamma = \dfrac{P_1 pl\big(d_{T_1,R_1}\big)}{N_1 + P_2 pl\big(d_{T_2,R_1}\big)} \end{cases}.$$

The packet corruption probability is calculated by the average bit error rate $E[e(\gamma_1)]$:

$$c_1 = 1 - \big(1 - E[e(\gamma_1)]\big)^{H_P + H_M + L}. \quad (3)$$

The channel idle probability is defined as follows. If T_1 can sense the transmission of T_2, then T_1 will consider the channel to be idle whenever T_2 is inactive, *i.e.*, $i_1 = 1 - \tau_2$; otherwise T_1 always senses the channel to be idle and $i_1 = 1$.

D. Loading Calculation

Suppose we want to schedule a flow of λ_n bits per second on (T_n, R_n), and ρ_n bits per second is achieved by (T_n, R_n), $n = 1, 2$. We refer λ_n and ρ_n to the *offered load* and the *carried load* respectively. We calculate ρ_n by

$$\rho_n = \frac{\tau_n (1 - c_n) L}{E[S_n]}, \quad (4)$$

where $E[S_n]$ is the expected length of a slot as seen by (T_n, R_n). Let a_n be the probability that at least one station is transmitting, and s_n be the probability that there is at least one successful transmission given that at least one station is transmitting. Then $E[S_n] = (1 - a_n)\sigma + a_n s_n (T_s + \sigma) + a_n(1 - s_n)(T_c + \sigma)$, where σ, T_s and T_c are the time spent in an idle slot, a successful transmission and an unsuccessful transmission respectively. When T_1 can sense the transmission of T_2, we consider both links to be one system:

$$\begin{aligned} a_1 &= 1 - (1 - \tau_1)(1 - \tau_2), \\ s_1 &= \frac{1 - [1 - \tau_1(1 - c_1)][1 - \tau_2(1 - c_2)]}{a_1}. \end{aligned}$$

Otherwise, we treat both links to be separate systems:

$$\begin{aligned} a_1 &= \tau_1, \\ s_1 &= 1 - c_1. \end{aligned}$$

We approximate the packet arrival of (T_n, R_n) to be a Poisson process with rate $\dfrac{\lambda_n}{L}$, $n = 1, 2$, and estimate the buffer nonempty probability by

$$q_n = 1 - \exp\left\{-\frac{\lambda_n}{L} E[S_n]\right\}. \quad (5)$$

E. Summary

In summary, if T_1 can sense the transmission of T_2, then we obtain the following set of equations for (T_1, R_1):

$$\begin{aligned} \tau_1 &= \left(2q_1^2 W_0 \sum_{j=0}^{m} c_1^j\right)\Bigg\{q_1^2 W_0 \sum_{j=0}^{m} c_1^j (W_j+1) \\ &\quad + (1-q_1)\Big[1-(1-q_1)^{W_0}\Big] \\ &\quad \times [q_1 \tau_2 (W_0+1) + 2(1-q_1)]\Bigg\}^{-1}, \\ c_1 &= 1 - [1 - e(\gamma_1)]^{H_P + H_M + L}, \\ q_1 &= 1 - \exp\Big\{-\big[\big(1 - [1 - \tau_1(1 - c_1)][1 - \tau_2(1 - c_2)]\big)T_s \\ &\quad + [\tau_1 c_1 + \tau_2 c_2 - \tau_1 \tau_2 (c_1 + c_2 - c_1 c_2)]T_c + \sigma\big]\frac{\lambda_1}{L}\Big\}. \end{aligned}$$

Otherwise, we obtain another set of equations for (T_1, R_1):

$$\tau_1 = \left(2q_1^2 W_0 \sum_{j=0}^{m} c_1^j\right)\Bigg\{q_1^2 W_0 \sum_{j=0}^{m} c_1^j (W_j + 1) + 2(1-q_1)^2\Big[1-(1-q_1)^{W_0}\Big]\Bigg\}^{-1},$$

$$c_1 = 1 - \big(1 - E[e(\gamma_1)]\big)^{H_P + H_M + L},$$

$$q_1 = 1 - \exp\Big\{-[\tau_1(1-c_1)T_s + \tau_1 c_1 T_c + \sigma]\frac{\lambda_1}{L}\Big\}.$$

Similarly, we can obtain three equations for link (T_2, R_2). With these six equations we can solve for the variables $\tau_1, c_1, q_1, \tau_2, c_2, q_2$ by Newton's method [16], and obtain the loadings of these two links by (4).

IV. Some Analytical Results

We use the two-ray ground reflection model

$$pl(d) = \frac{G_t G_r h_t^2 h_r^2}{d^4} = \frac{C}{d^4}$$

to represent the path loss, where G_t and G_r are the gain of transmitter and receiver antenna respectively, h_t and h_r are the height of transmitter and receiver antenna respectively, and $C = G_t G_r h_t^2 h_r^2$. The path loss exponent is 4. We use the values in Table I to obtain numerical results from our model. These values are defined in or derived from the values in the 802.11 MAC and PHY specifications [13] or NS-2 [17].

In the following we attempt to find the maximum carried loads of each link in various scenarios. One observation from solving the system of equations in Section III is that the carried load will be smaller than the offered load when the offered load is too large. This corresponds to the instability of 802.11 observed in previous works (*e.g.*, [7]). Therefore, we use binary search to find the maximum carried load under stable conditions. Initially, the search range for the offered load is between 0 and 1Mbps. We choose the midpoint of the search range to be the offered load and solve the system of equations. If the resultant carried load is the same as the offered load, the offered load can be increased and the next search range will be the upper half of the original one. Otherwise, the offered load results in instability and the next search range will be the lower half of the original one. This procedure is repeated until the search range is sufficiently small.

We consider a network of two parallel links as shown in Fig. 2, with d and r representing the length of the links and the link separation respectively. The link separation is defined as the perpendicular distance between the links. We let $L = 8192$ bits, $d = 450$ meters, and $\beta = -70, -75, -78, -80$ dBm to solve for the maximum carried loads and obtain the curves as shown in Figs. 3(a)-3(d).

Consider the curve corresponding to the carrier sensing threshold of -78 dBm in Fig. 3(c), which is a common value used in NS-2 simulation and the practical value used in Orinoco wireless LAN card. The corresponding carrier sensing range is 550 meters, which is in line with the carrier sensing range used in practice. In our model, we assume that carrier sensing works when the separation is within the carrier sensing range and fails otherwise, and use two different sets of equations to model the system in these situations. Therefore there is an abrupt change in the aggregate throughput when the separation equals the carrier sensing range. If there is no carrier sensing in the system, the aggregate throughput will reduce to zero smoothly when the link separation reduces.

TABLE I

Parameters used for the analytical results.

H_P	192 bits	H_M	272 bits
m	7	m'	5
W_0	32	σ	20 μs
T_s	9020 μs	T_c	9020 μs
P_1, P_2	24.5 dBm	N_1, N_2	-88 dBm
G_t, G_r	1	h_t, h_r	1.5 m

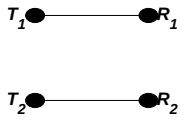

Fig. 2. A sample topology.

The curve in Fig. 3(c) can be divided into three parts according to the link separation r. When $r < 550$ meters, both transmitters are in the carrier sensing range of each other. As a result, at most only one transmitter is active at a time. If $r \geq 550$ meters, the transmitters are unaware of the existence of each other, and they contend for the wireless channel as if there were no interferers nearby. When $r > 800$ meters, the separation is so large that there will not be any interference between the links. When r lies between 550 and 800 meters, the aggregate throughput of the links increases smoothly as r increases. We label this range of r as the *partial interference region*. The existence of this partial interference region suggests that the interference models proposed by [1] that a single threshold can represent the interference relationship in wireless networks may be overly simplified.

The width of this partial interference region depends on the carrier sensing threshold β used. Smaller values of β, *e.g.*, -80 dBm, result in a narrower partial interference region as in Fig. 3(d). Simultaneous transmissions are allowed only for the links separated far enough, and the throughput is suppressed significantly. For larger β, *e.g.*, -75 and -70 dBm, more *spatial reuse* is allowed, and the width of the partial interference region is larger, as shown in Figs. 3(a)-3(b). However, excessive interference is introduced for larger β, so there is a reduction in the aggregate throughput.

Besides carrier sensing threshold, the length of the links d also affects the partial interference region. We reduce d to be 400 meters, and obtain the results in Figs. 4(a)-4(d). As shown in Figs. 4(a)-4(d), the partial interference region becomes narrower for all values of carrier sensing threshold. Also, the aggregate throughput achieved by the links is larger for the same link separation when the links are shortened.

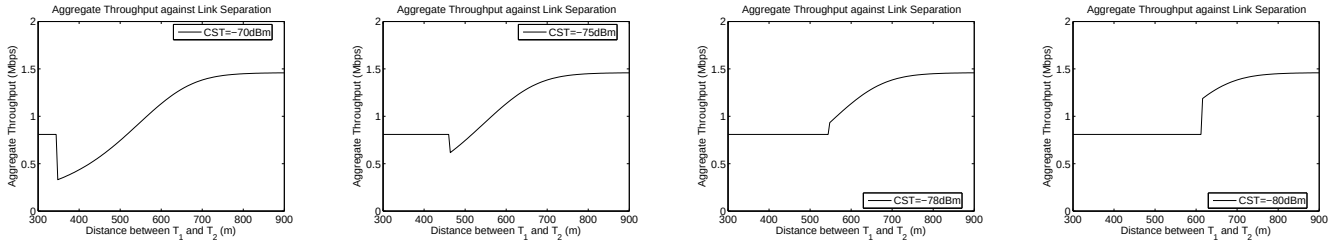

(a) (b) (c) (d)

Fig. 3. Aggregate throughput for the topology in Fig. 2 with length of links = 450 meters and carrier sensing threshold = (a) -70 dBm, (b) -75 dBm, (c) -78 dBm and (d) -80 dBm.

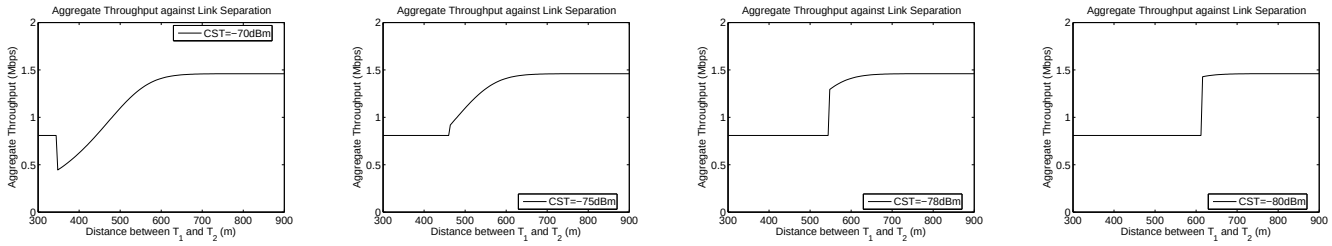

(a) (b) (c) (d)

Fig. 4. Aggregate throughput for the topology in Fig. 2 with length of links = 400 meters and carrier sensing threshold = (a) -70 dBm, (b) -75 dBm, (c) -78 dBm and (d) -80 dBm.

Next we compute the *admissible region* predicted from our model. The admissible region includes all the points (λ_1, λ_2) such that if (λ_1, λ_2) is located inside the admissible region, then a flow of λ_n can be allocated on and achieved by (T_n, R_n), $n = 1, 2$. We use the same settings as above, and choose the carrier sensing threshold to be -78 dBm. The link separations are chosen to be 500, 600 and 900 meters for illustrative purposes, because they correspond to different shapes of the admissible region. Fig. 5 shows the admissible region for these three link separations. The link separation of 500 meters represents that the links are in mutual interference, and the admissible region has a triangular shape. When the links are separated by 900 meters, the links do not interfere with each other, and the admissible region is rectangular. For the link separation of 600 meters, partial interference exists and the admissible region becomes convex.

V. A TDMA/CDMA Analogy

In this section, we use TDMA, CDMA and Shannon's capacity to establish an analogy to our results in Section IV. Consider the same network as in Fig. 2. The bandwidth of the channel is denoted by B.

If the links use TDMA as the multiplexing scheme to share the wireless channel, then only one link can be active at a time. So there is no interference, and the SNR at the receiver of each link is $\gamma = \dfrac{PCd^{-\alpha}}{N}$. Then by Shannon's capacity formula [15], the aggregate capacity is

$$\rho_{TDMA} = B \log_2(1 + \gamma).$$

If CDMA is used instead, then the SNR at the receiver of each link will be $\dfrac{PCd^{-\alpha}}{N + PC(d^2 + r^2)^{-\frac{\alpha}{2}}} = \dfrac{1}{\gamma^{-1} + z}$, where $z = \left(\dfrac{d^2}{d^2 + r^2}\right)^{\frac{\alpha}{2}}$. The aggregate capacity is

$$\rho_{CDMA} = 2B \log_2\left(1 + \frac{1}{\gamma^{-1} + z}\right).$$

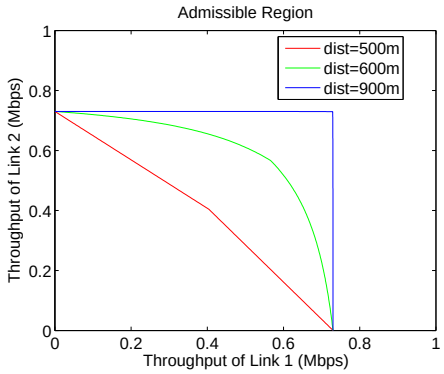

Fig. 5. Admissible region for various link separations.

Fig. 6 shows the variation of aggregate capacity against link separation in TDMA and CDMA, normalized by the capacity in TDMA, with $d = 450$ meters. The aggregate capacity is independent of the link separation in TDMA, and increases smoothly with the link separation in CDMA. There exists a crossover point r_0 such that, when $r < r_0$, TDMA has a higher aggregate capacity, and the opposite occurs otherwise. The notion of setting a carrier sensing threshold or range can be viewed as deciding when to *switch* between TDMA and

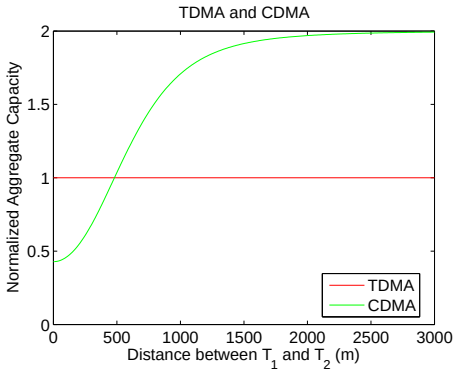

Fig. 6. A TDMA/CDMA analogy for the results in Section IV.

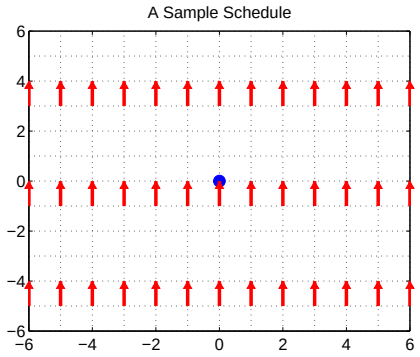

Fig. 7. A scheduling pattern in the modified Manhattan network.

CDMA: use TDMA when the separation is smaller than the carrier sensing range, use CDMA otherwise. Carrier sensing allows at most one link to be active at a time, so the links within carrier sensing range share the wireless channel like TDMA. Partial interference is analogous to CDMA that the aggregate throughput increases smoothly as the link separation increases. We can obtain the behavior in Section IV by setting the carrier sensing range to be close to r_0, and achieve optimal performance in terms of aggregate capacity by setting the carrier sensing range to be r_0.

VI. Capacity Gain by Exploiting Partial Interference

In this section, we demonstrate that there is a gain in capacity by exploiting partial interference. We consider one variation of the Manhattan network [11], *i.e.*, a network consisting of a rectangular grid extending to infinity in both dimensions. The horizontal and vertical separation between neighboring stations are denoted by r and d respectively. The capacity of each link without interference is denoted by ρ_0.

We assume DBPSK is employed and a packet consists of L bits. We use the two-ray ground reflection model for path loss as in Section IV. To apply the physical model in [1], we let the SNR threshold γ_0 be the case that the packet error rate is ϵ, *i.e.*, $1-\left[1-\frac{1}{2}\exp(-\gamma_0)\right]^L = \epsilon$. We let $L = 8192$ and $\epsilon = 10^{-3}$, therefore the SNR requirement is $\gamma_0 = 15.23$. Assuming there is no interferer, this SNR requirement is met when the length of a link is smaller than 493 meters.

We use a Cartesian coordinate plane to represent the modified Manhattan network. One station is placed at every point with integral coordinates in the network. Suppose we schedule flows in the modified Manhattan network from the South to the North using the pattern shown in Fig. 7 and its shifted versions. In Fig. 7, an arrow is used to represent an active link, where the tail and the head of an arrow denote the transmitter and the receiver of the link respectively.

We use the *capacity across unit cut* $\eta(\mu)$ as the performance metric, where $\mu = \frac{r}{d}$ is the ratio of the horizontal separation to the vertical separation. It is a measure on how much we can send through a cut on average while packing the links together. Consider the SNR attained at the receiver marked with the blue circle, which has the position assigned as the origin in the Cartesian coordinate plane. The SNR is defined by $\gamma(\mu) = \frac{S}{N+I(\mu)}$, where S is the received power from the intended transmitter and $I(\mu)$ is the power received from all interferers. The capacity achieved by each link is $\rho(\mu) = \rho_0\left\{1-\frac{1}{2}\exp[-\gamma(\mu)]\right\}^L$ under partial interference; while in the physical model, we let $\rho(\mu) = \rho_0$ if $\gamma(\mu) \geq \gamma_0$ and $\rho(\mu) = 0$ otherwise. A *cut* $\mathcal{C}$ in the network is an infinitely long horizontal line. Let $\{T_n\}_{n\in\mathbb{N}}$ be the set of all active transmitters such that $\mathcal{C}$ intersects the link used by T_n. We divide $\mathcal{C}$ into segments $\mathcal{C}(T_n), n \in \mathbb{N}$, where

$$\mathcal{C}(T_n) = \left\{x \in \mathcal{C} \colon \|x - T_n\| = \min_{n'\in\mathbb{N}} \|x - T_{n'}\|\right\}$$

and $\|\cdot\|$ is the Euclidean norm. Then the length $\mathcal{L}$ of the cut occupied by an active transmitter is the length of $\mathcal{C}(T_n)$, and the capacity across unit cut is therefore $\eta(\mu) = \frac{F\rho(\mu)}{\mathcal{L}}$, where F is the fraction of time that a link is active.

In the following we assume $d = 450$ meters. For the schedule in Fig. 7, the signal power is $S = \frac{PC}{d^4}$. All the transmitters in Fig. 7 are located at positions $(x, 4y-1)$, where x and y are integers. The interference power is

$$\begin{aligned} I(\mu) &= \left\{\sum_{x=-\infty}^{\infty}\sum_{y=-\infty}^{\infty} \frac{PC}{\left((xr)^2 + [(4y-1)d]^2\right)^2} - \frac{PC}{d^4}\right\} \\ &= \left\{\sum_{x=-\infty}^{\infty}\sum_{y=-\infty}^{\infty} [(x\mu)^2 + (4y-1)^2]^{-2} - 1\right\}\frac{PC}{d^4}. \end{aligned}$$

Considering the physical model, if the schedule is allowed to be active, we need $\mu \geq \mu_0 = 5.58$, as listed in Table II and depicted in Fig. 8 by the blue dashed line. The value of μ_0 is obtained from $\gamma(\mu_0) = \gamma_0$. Each active transmitter occupies a cut of length $r = \mu d$ and each link is active for one quarter of a cycle. Therefore, for $\mu = \mu_0$, the maximum capacity across unit cut under the physical model is $\frac{\rho_0}{4\mu_0 d} = 0.0996\rho_0$ bits per second per kilometer.

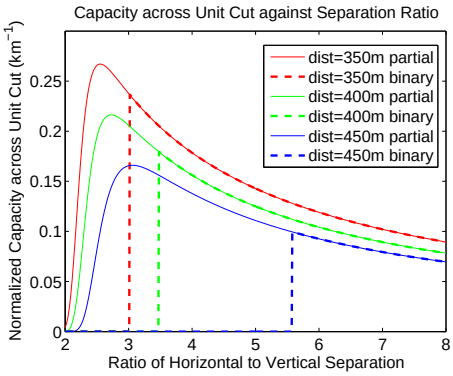

Fig. 8. Capacity across unit cut for different length of links under the physical model (binary interference) and partial interference.

TABLE II

CAPACITY GAIN IN THE MODIFIED MANHATTAN NETWORK WITH DIFFERENT LENGTH OF LINKS.

d	μ_0	$\eta(\mu_0)$	μ_{opt}	$\eta(\mu_{opt})$	% increase
350	3.02	0.2365 ρ_0	2.55	0.2671 ρ_0	12.93%
400	3.48	0.1796 ρ_0	2.73	0.2163 ρ_0	20.45%
450	5.58	0.0996 ρ_0	3.06	0.1661 ρ_0	66.82%

If we allow partial interference, the active transmitters can be packed more closely. When μ decreases, more spatial reuse is allowed. The increase in the density of active transmitters outweighs the degradation in capacity, so there is an increase in the capacity across unit cut. However, if μ decreases further, interference will be the dominant factor in determining the capacity across unit cut. Therefore, the capacity across unit cut drops, and there exists μ_{opt} for the optimal performance under partial interference. This behavior is depicted by the blue solid line in Fig. 8. The optimal value of μ under partial interference is $\mu_{opt} = 3.06$, and the capacity across unit cut is $0.1661\rho_0$ bits per second per kilometer. There is a percentage increase of 66.82% in the capacity across unit cut by exploiting partial interference. Similar results are shown in Table II and Fig. 8 for $d = 350, 400$ meters. The percentage increase is larger when the links are longer, but the capacity achieved by each link reduces. We can view $\mu_0 d$ as the carrier sensing range in the modified Manhattan network with the scheduling pattern in Fig. 7, as it is the smallest horizontal separation allowed by the physical model. We observe that if the length of the links increases, the carrier sensing range needs to be increased in a larger proportion. Also, this carrier sensing range is much larger than double of the length of the links, which is the usual convention used in defining the relationship between carrier sensing range and transmission range.

VII. CONCLUSION

In this paper, we have presented an analytical framework to characterize the partial behavior of interference in a wireless network. We observed that the threshold-based protocol and physical models may not be accurate enough to model the interference in a wireless network. We noticed the importance of carrier sensing threshold through the results of our analytical model and established an analogy between partial interference and CDMA. We also demonstrated that there is a gain in capacity by considering partial interference in the modified Manhattan network.

In view of this work, one of the possible future works is to consider partial interference when computing the capacity of a wireless network. We may modify the interference constraints in [2], [3] and [4] to take into account partial interference, and evaluate how much will be gained by considering partial interference in scheduling in wireless networks. Another possibility is to consider the capacity-finding problem with random access MAC protocols like 802.11. This can be used to provide QoS guarantees without assuming the existence of perfect global schedulers as in [2], [3] and [4], therefore it does not require modifying existing MAC protocols. Also, we may extend our framework to consider partial interference in wireless networks with multiple partially overlapped channels.

REFERENCES

[1] P. Gupta and P. R. Kumar, "The Capacity of Wireless Networks," *IEEE Trans. Inform. Theory*, vol. 46, no. 2, pp. 388–404, Mar. 2000.

[2] K. Jain, J. Padhye, V. Padmanabhan, and L. Qiu, "Impact of Interference on Multi-hop Wireless Network Performance," in *MobiCom 2003*, San Diego, California, USA, Sept. 2003.

[3] R. Gupta, J. Musacchio, and J. Walrand, "Sufficient Rate Constraints for QoS Flows in Ad-Hoc Networks," *Ad Hoc Networks*, 2006.

[4] M. Kodialam and T. Nandagopal, "Characterizing the Capacity Region in Multi-Radio Multi-Channel Wireless Mesh Networks," in *MobiCom 2005*, Cologne, Germany, Aug./Sept. 2005.

[5] J. Padhye, S. Agarwal, V. N. Padmanabhan, L. Qiu, A. Rao, and B. Zill, "Estimation of Link Interference in Static Multi-hop Wireless Networks," in *Internet Measurement Conference*, Berkeley, CA, Oct. 2005.

[6] A. Mishra, E. Rozner, S. Banerjee, and W. Arbaugh, "Exploiting Partially Overlapping Channels in Wireless Networks: Turning a Peril into an Advantage," in *Internet Measurement Conference*, Berkeley, CA, Oct. 2005.

[7] G. Bianchi, "Performance Analysis of the IEEE 802.11 Distributed Coordination Function," *IEEE J. Select. Areas Commun.*, vol. 18, no. 3, pp. 535–547, Mar. 2000.

[8] R. K. Ahuja, T. L. Magnanti, and J. B. Orlin, *Network Flows: Theory, Algorithms and Applications*. Prentice Hall, 1993.

[9] S. J. Shellhammer, "Estimation of Packet Error Rate Caused by Interference using Analytic Techniques - A Coexistence Assurance Methodology," IEEE 802.19 Technical Advisory Group Document Archive, Qualcomm, Inc., Oct. 2005.

[10] W. Luo and A. Ephremides, "Stability of N Interacting Queues in Random-Access Systems," *IEEE Trans. Inform. Theory*, vol. 45, no. 5, pp. 1579–1587, July 1999.

[11] G. Mergen and L. Tong, "Stability and Capacity of Regular Wireless Networks," *IEEE Trans. Inform. Theory*, vol. 51, no. 6, pp. 1938–1953, June 2005.

[12] H. Wu, Y. Peng, K. Long, S. Cheng, and J. Ma, "Performance of Reliable Transport Protocol over IEEE 802.11 Wireless LAN: Analysis and Enhancement," in *INFOCOM 2002*, June 2002.

[13] *Wireless LAN Medium Access Control (MAC) and Physical Layer (PHY) Specifications*, IEEE Std. 802.11, 1999.

[14] D. Malone, K. Duffy, and D. J. Leith, "Modeling the 802.11 Distributed Coordination Function in Non-saturated Heterogeneous Conditions," *IEEE/ACM Trans. Networking*, vol. 15, no. 1, 2007.

[15] T. S. Rappaport, *Wireless Communications: Principles and Practice*, 2nd ed. Prentice Hall, 2002.

[16] D. Kincaid and W. Cheney, *Numerical Analysis: Mathematics of Scientific Computing*, 3rd ed. Brooks/Cole, 2002.

[17] The Network Simulator - ns-2. [Online]. Available: http://www.isi.edu/nsnam/ns/